

Topological monopoles and currents in electromagnetic waves

Vladlen Shvedov¹, Wieslaw Krolikowski^{1,2}

¹*Laser Physics Centre, Research School of Physics and Engineering,
Australian National University, Canberra, ACT 0200, Australia*

²*Science Program, Texas A&M University at Qatar, Doha, Qatar*

Singularities, i.e. places of discontinuities of parameters are extremely general objects appearing in electromagnetic waves and thus are the key to understanding fundamental wave processes. These structures commonly occur in purely coherent, highly directional waves, such as laser beams, determining additional spatial or "topological" properties of the wave fields independently of their propagational dynamics. For instance, topologies of wave fronts, called phase singularities, add orbital degrees of freedom to electromagnetic waves. These singularities are common to all types of scalar waves described only by their intensity and phase distributions. As the electromagnetic wave is a vector wave, its topological properties generally depend on all field components leading to complex field patterns in space and time. These patterns may contain singular points of undefined instantaneous orientation of the vector field, i.e. the instantaneous field (IF) singularities. In zero-order paraxial approximation of purely transverse electromagnetic waves, some instantaneous field distributions may carry apparent topological monopoles, when the originally source-free wave exhibits spatial structure associated with the 2D "virtual" sources of electromagnetic fields.

Here we present systematic description of topological singularities in both electric and magnetic field of the electromagnetic waves in a paraxial approximation. We also consider the important types of paraxial electromagnetic waves with complex transverse field structures containing instantaneous field singularities.

INTRODUCTION

The traditional approach to describe propagating electromagnetic radiation in free space is based on the differential form of Maxwell's electromagnetic theory and the corresponding wave equation [1]. This approach gives a detailed account of electromagnetic waves as synchronized transverse oscillations of electric and magnetic fields satisfying the superposition principle at a point. As result, all fundamental wave parameters, such as amplitude, wave frequency, direction in space (wave vector), orientation of fields (polarization) and phase refer to behavior of the wave at a particular point in space and time. This representation of electromagnetic wave via only local "at point" parameters is perfect from the fundamental point of view on condition that the wave field is free of physical discontinuities. There is no doubt that the local wave parameters can be different at different points of the wave [2-10] even in purely coherent and highly directional electromagnetic radiations, such as paraxial laser beams [11-13]. It is also true that as the state of the wave field changes, the parameters may not always be defined throughout space. Typically, there are some particular points in the wave field where the local parameters, such as the phase, state and handedness of the polarization or orientation of electric (magnetic) vectors are not defined [4]. These points are known as singularities in the wave field [14]. As all certain values of a singular parameter in the wave occur in the neighbourhood of a singular point (but not in the point itself), singularities define spatial properties of the surrounding wave field [9]. This requires one to deal with additional "integral" characteristics describing spatial "topological" properties of the

wave field [4, 5]. They are related to the fundamental geometrical aspects of electromagnetic waves and are associated with the inhomogeneous distributions of local parameters, such as the phase and electric (magnetic) vector orientation, which constitute the wave singularities. These singularities are typically classified as phase and polarization singularities, depending on which parameter is undefined (or singular) at some points in the wave. Phase singularities, commonly known in light fields as "optical vortices" [15], are features of scalar components of vectorial electromagnetic waves, leading to a circulation of the electromagnetic energy around the point in two dimensions [16-19]. They also occur naturally for all types of scalar waves, both classical and quantum [20, 21], and have been studied in detail in a number of works in the different branches of wave physics [see, for instance vortices in electron beams [22-24].

Other types of singularities may occur in electromagnetic waves when the vectorial properties of the waves cannot be ignored. Well known are the polarization singularities that naturally appear in completely polarized electromagnetic waves where the state of polarization varies with position, first described in detail by J. Nye [25, 26]. They refer to the points where the direction of the polarization or the handedness of the polarization ellipse is not defined [9, 25]. As the state of polarization is actually determined by electromagnetic vectors averaged over the period of wave oscillations, the polarization pattern alone cannot properly expose the deep nature of singularities in these fields. The polarization provides only rough and, sometimes, distorted picture of instantaneous orientation of electric vectors in the vicinity of a singular point in the vector wave. The simplest

example is a vector field of a uniformly circularly (generally elliptically) polarized optical vortex which cannot be properly explained in terms of either pure phase or polarization singularities, as we will show in Section 2. On the other hand, the instantaneous orientations of electromagnetic vectors in the wave field provide a natural and efficient way to describe the most fundamental features of physical discontinuities in paraxial vector waves. Corresponding instantaneous vector field (IF) singularities are not stable, but exhibit periodic evolution in propagation in space as the field vectors oscillate in time. These special IF singularities are source of unique 2D field structures which we call *wave monopoles* and *wave currents* in transverse components of the wave. We will consider them in detail in Section 3. Then, in Section 4, we will discuss wave fields with mixed topology and polarization singularities. To clarify the concept of IF singularities, we will start from the general principles of electromagnetic wave topology and its trivial cases of homogeneously (generally elliptically) polarized fields and then we will move on to more complex scenarios involving scalar and vector singularities in the waves. Moreover, we consider here only electromagnetic waves which carry finite energy flux and are self-similar in space. The former leads to spatially localized waves in the form of light beams. The latter means that the intensity of the beam is similar in each plane S_{\perp} orthogonal to the propagation direction.

PARAXIAL MODEL OF ELECTROMAGNETIC BEAMS

In general, the electromagnetic fields \mathbf{E} , \mathbf{B} in a free propagating wave are complicated functions of both space and time. The situation becomes simpler for monochromatic harmonic waves with constant frequency ω , where one can naturally separate spatial and time dependences. In many practical cases, this allows one to describe a harmonic wave as a product of complex-valued spatial mode and a complex exponential of time, remembering to take the real part to obtain the physical fields: $\{\mathbf{E}, \mathbf{B}\} = \text{Re}\{\mathbf{F}(x, y, z)e^{-i\omega t}\}$. Description of spatial modes is based on the spatially invariant Helmholtz wave equation (which in turn is derived from differential form of Maxwell equations)

$$(\nabla^2 + k^2)\mathbf{F} = 0, \quad (1)$$

where $\nabla = \mathbf{e}_x\partial_x + \mathbf{e}_y\partial_y + \mathbf{e}_z\partial_z$, $\partial_u \equiv \partial/\partial u$, $u=x, y, z$, and $\mathbf{e}_x, \mathbf{e}_y, \mathbf{e}_z$, are the unit vectors in Cartesian coordinates, $k = \omega/c$ is a wave number, c is speed of light, and \mathbf{F} represents electric or magnetic field, respectively. When the electromagnetic radiation is a highly directional along a certain spatial axis (for example, z), a spatial mode can be expressed as $\mathbf{F}(x, y, z) = \tilde{\mathbf{F}}(x, y, z)e^{ikz}$ with a complex

amplitude $\tilde{\mathbf{F}}(x, y, z)$ satisfying to the spatially asymmetric equation

$$(\nabla^2 + 2ik\partial_z)\tilde{\mathbf{F}} = 0. \quad (2)$$

As was shown by M. Lax *et al.* [27], in the zero-order paraxial approximation, the electromagnetic field are purely transverse $\tilde{\mathbf{F}} = \mathbf{F}_{\perp}$ and the second z -derivative could be ignored in the Eq.(2) with respect to a slowly-varying first z -derivative of the amplitude function \mathbf{F}_{\perp} . Finally, the equation for the complex amplitude takes form of a parabolic equation:

$$(\nabla_{\perp}^2 + 2ik\partial_z)\mathbf{F}_{\perp} = 0, \quad (3)$$

where $\nabla_{\perp} = \mathbf{e}_x\partial_x + \mathbf{e}_y\partial_y$.

Note that the transversality of the field breaks down in the next order correction [27]. By analysing the higher-order terms in the series expansion of Maxwell's equations, Lax found that the first-order terms of expansion has a small longitudinal field component and its value is obtained from the transverse components through the relation $kF_z = i\nabla_{\perp}\mathbf{F}_{\perp}$. The role of longitudinal components in the next order of the paraxial approximation will be discussed in sections 4 and 5. Here, our main interest is the zero-order paraxial approximation as the basis to clarify the topology and field singularities phenomena in the coherent electromagnetic waves. A scalar form of the Eq. (3) is represented by a parabolic equation of the Schrödinger type that describes the complex amplitude of a Cartesian component $F_{\perp} = F_{x,y}$ of the electromagnetic wave

$$\nabla_{\perp}^2 F_{\perp} = -2ik\partial_z F_{\perp}. \quad (4)$$

This equation admits solutions in a form of self-similar beams preserving their structure in propagation [28]. Many of such solutions with both, infinite and finite energies, have been obtained in the last decades [13, 29-36]. Main attention has been paid to the spatially-localized solutions with finite energy flux [29-35] as the only ones having physical sense. They include, among others, the well-known Hermite-Gaussian and Laguerre-Gaussian beams; elegant and generalized Laguerre-Gaussian beams; Bessel-Gauss beams; hypergeometric-Gauss beams; fractional-order elegant Laguerre-Gaussian beams; Bessel-Gauss beams with quadratic radial dependence; Mathieu and Ince-Gaussian beams, and optical vortex beams (see [36] and references therein).

As indicated by their names, all spatially localized characteristics of such beams are predominantly associated with the Gaussian envelope

$$G(x, y, z) = \frac{1}{\xi(z)} \exp\left(-\frac{\rho^2}{w_0^2\xi(z)}\right), \quad (5)$$

where $\rho = \sqrt{x^2 + y^2}$ is the radial coordinate of an arbitrary point, $\xi(z) = 1 + iz/z_0$, $z_0 = kw_0^2/2$ and w_0 is a beam waist in the plane $z = 0$.

The scalar function G is extremely important in understanding paraxial electromagnetic wave behavior because it serves as a background envelope for more general wave solutions, ensuring finiteness of their energy as $\int_0^\infty (2/\pi w_0^2) G G^* dS_\perp = 1$ (the star denotes complex conjugation).

The general, rigorous solutions to the parabolic equation (2) can be represented as a product [38]

$$\mathbf{F}_\perp = \mathbf{U}(x, y, z)G(x, y, z), \quad (6)$$

where $\mathbf{U}(x, y, z)$ is a complex vector modulating function and $G(x, y, z)$ is of the form of Eq.(5). While the Gaussian amplitude describes evolution of the localized envelope of scalar waves or beams in space, the modulation function \mathbf{U} determines their all topological and vector properties. Despite the infinite number of possible modulation functions \mathbf{U} , their general structure can be defined by just a few basic topological properties. Therefore, in the following we will concentrate on the functions \mathbf{U} having the most typical topological properties. However, before going any further, let us clarify the relevant terminology.

As the functions \mathbf{U} are vector fields defining the orientation of electric (magnetic) fields in space, they are directly related to the state of polarization of the beams. Typically, only beams with spatially variant polarization in their transverse cross-sections are deemed vector beams. In contrast, beams with a constant polarization are generally considered as scalar.

At this point, it is worth clarifying the relationship between the state of polarization and field orientation as these two terms that are often, yet incorrectly, used interchangeably. The state of polarization is a time-averaged parameter of a beam and, so far, can be purely homogeneous while the instantaneous orientation of electric (magnetic) vectors provides a complex pattern in the transverse cross-section of the beam. In such cases, the electromagnetic fields of the beam are solutions to the full vector wave equation, and cannot be defined by one scalar function. According to superposition principle, it is always possible to present the transverse vector function \mathbf{U} (corresponding to \mathbf{E} or \mathbf{B} fields) in terms of their Cartesian components:

$$\mathbf{U} = A_x U_x(x, y, z)\mathbf{e}_x + A_y U_y(x, y, z)\mathbf{e}_y, \quad (7)$$

where A_x and A_y are arbitrary, generally complex constants.

We consider the beam to be a “scalar” when its electromagnetic field can be described by the real part of a single scalar modulating function:

$$\frac{Re\{A_x U_x\}}{Re\{A_x\}} = \frac{Re\{A_y U_y\}}{Re\{A_y\}} = Re\{U\}, \quad (8)$$

In case of a “vector beam” the transverse Cartesian components of the modulating function (7) $\mathbf{U}_x = A_x U_x(x, y, z)$

\mathbf{e}_x , and $\mathbf{U}_y = A_y U_y(x, y, z)\mathbf{e}_y$ depend in different way on coordinates:

$$\frac{Re\{A_x U_x\}}{Re\{A_x\}} \neq \frac{Re\{A_y U_y\}}{Re\{A_y\}}, \quad (9)$$

The simplest example of the scalar beam is an elliptically polarized Gaussian beam. This trivial case occurs if the modulating function is constant: $\mathbf{U} = A_x \mathbf{e}_x + A_y \mathbf{e}_y$, where $A_x = a_x$ and $A_y = a_y e^{i\phi}$; a_x and a_y are real numbers and ϕ is the phase difference between Cartesian components of \mathbf{U} . Then one immediately obtains the simplest solution of Eq.(2) in form of complex amplitude $\mathbf{F}_\perp = (a_x \mathbf{e}_x + a_y e^{i\phi} \mathbf{e}_y)G$ of the elliptically polarized beam $\mathbf{F}_\perp e^{i(kz - \omega t)}$, which certainly is a scalar wave. This paraxial, fundamental Gaussian beam [11-13], is only one of the infinite numbers of possible variations of electromagnetic beams described by Eq. (6). However, homogeneous distributions of instantaneous electric (magnetic) field vectors with the same orientation at each point of the transverse plane of beams is a sufficiently rare. Generally, beams have complex distributions of phase, polarization or the instant directions of the electromagnetic fields changing from point to point in the transverse plane.

In the next Section, we will provide examples of scalar and vector beams with nontrivial topology of modulating functions.

SCALAR AND VECTOR BEAMS WITH TOPOLOGICAL CHARGES

In general, the function $\mathbf{U}(\rho, \varphi, z)$ depends on all three coordinates. By changing variables as $R_t = \sqrt{X^2 + Y^2} = \rho/(w_0 \xi)$, where $X = x/(w_0 \xi)$; $Y = y/(w_0 \xi)$, following standard procedure shown in works [34, 38], we insert expression (6) into wave equation (2) and obtain differential equation for the modulating function $\mathbf{U}(R_t, \varphi, \xi)$ in the form

$$\nabla_t^2 \mathbf{U} - 4\xi^2 \partial_\xi \mathbf{U} = 0 \quad (10)$$

where $\nabla_t = \mathbf{e}_x \partial_X + \mathbf{e}_y \partial_Y$.

This equation admits the separation of variables

$$\mathbf{U}(R_t, \varphi, \xi) = \mathbf{u}(R_t, \varphi)Z(\xi), \quad (11)$$

where the function $Z(\xi) = \exp(K^2(1 - \xi)/4\xi)$, and K is a constant. Then the function $\mathbf{u}(R_t, \varphi)$ satisfies the two dimensional vector Helmholtz equation

$$(\nabla_t^2 + K^2) \mathbf{u} = 0. \quad (12)$$

In order to analyze possible solutions of Eq. (12) let us start with an important particular case when the constant K is equal to zero and, hence $Z = 1$. Then the

modulation function \mathbf{U} is independent of the longitudinal coordinate ξ and $\mathbf{U}=\mathbf{u}$. In this case, the vector Helmholtz equation (12) reduces to the vectorial Laplace equation for the function $\mathbf{U}(R_t, \varphi)$

$$\nabla_t^2 \mathbf{U}(R_t, \varphi) = 0. \quad (13)$$

Components U_x and U_y of the modulating function \mathbf{U} are, in general, independent scalar functions, interpreted as complex amplitudes of electromagnetic waves along Cartesian coordinates x and y , respectively. When the polarization state of the light field is homogenous (generally elliptical), the modulating function \mathbf{U} can be represented by a single scalar functions $U_x(x, y, z)=U_y(x, y, z)=U(x, y, z)$ as

$$\mathbf{U} = (a_x \mathbf{e}_x + a_y e^{i\phi} \mathbf{e}_y) U, \quad (14)$$

where U satisfies to the two-dimensional Laplace equation

$$\nabla_t^2 U = 0 \quad (15)$$

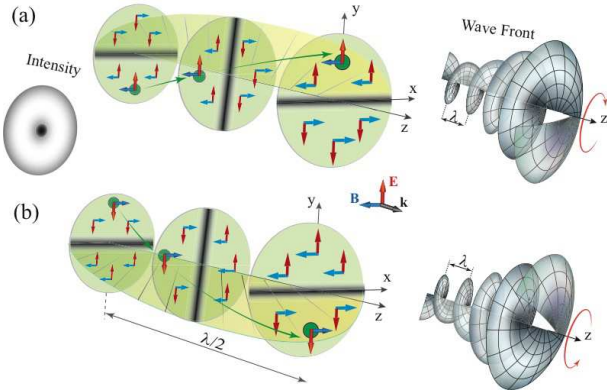


FIG. 1. The instantaneous, near-axis distribution of the electromagnetic fields and wave front of the scalar, linearly polarized vortex with topological charge $l = +1$ (a) and $l = -1$ (b). Each point of the wave's surface (see green circle) follows a spiral trajectory around the axis of the beam as the latter propagates.

From the spectrum of possible solutions of Eq. (15), well known as harmonic functions [39], we will consider the simplest but critically important solutions which play a key role in classification of light singularities in scalar light beams

$$U(R_t, \varphi) = R_t^n \exp(isn\varphi), \quad (16)$$

where $n = 0; \pm 1; \pm 2 \dots$, and $s = \pm 1$.

The function (16) has singularity on the line $R_t=0$ when $n \neq 0$, and its modulus on this line is either 0 for $n > 0$ or ∞ for $n < 0$. Finite energy solution (6) with modulation function (16) can be realized for $n \geq 0$, except for

some specific superpositions in which the self-similarity of the resulting light beam is lost [40]. Then the product sn in an exponent of Eq.(16) can be represented by a new integer $l = 0; \pm 1; \pm 2 \dots$, and order n in R_t becomes $n = |l|$, when $n \geq 0$. The physical solutions now read

$$U(R_t, \varphi) = R_t^{|l|} \exp(il\varphi). \quad (17)$$

While the harmonic function (17) is the simplest solution of Eq. (15) it gives full information about the topological structure in the field's components. The azimuthal index l defines the topological structure of the wave surface. In optics this index is named a topological charge of an optical vortex. The term "optical vortex" refers to the general solution (6) with scalar modulation functions containing addend $l\varphi$ in its phase, $\theta(\rho, \varphi, z)$. Then the wave front of the optical vortex has a form of a helicoid-like surface twisted around the singular line $R_t = 0$. Moreover, the phase circulating around the singularity line in the function (17) results in phase discontinuity that is multiple of the topological charge

$$\oint d\theta = \oint \nabla\theta d\mathbf{l} = 2\pi l, \quad (18)$$

where $d\mathbf{l}$ is the infinitesimal vector element of the loop. Consequently, the directional electromagnetic wave with the modulating function (17) carries discrete angular momentum [5] along the propagation axis z

$$M_z = \langle U^* | L_z | U \rangle / \langle U^* | U \rangle = l\hbar, \quad (19)$$

where $L_z = -i\hbar\partial/\partial\varphi$ is the generator of rotations around z .

The above discussed features apply to any scalar modulating functions with the singular phase factor $l\varphi$.

In general, the scalar Cartesian components of the function $\mathbf{u}(R_t, \varphi)$ in Eq. (11) satisfy the two-dimensional Helmholtz equation (12) which takes a scalar form

$$(\nabla_t^2 + K^2) u = 0. \quad (20)$$

Among an infinite number of possible solutions of Eq. (20) there are axially symmetric solutions with the phase topology similar to (17)

$$u(R_t, \varphi) = J_{|l|}(KR_t) \exp(il\varphi) \quad (21)$$

where $J_l(x)$ is the l -order Bessel function of the first kind. The corresponding scalar components of modulating function (11) are

$$U(R_t, \varphi, \xi) = J_{|l|}(KR_t) Z(\xi) \exp(il\varphi). \quad (22)$$

These functions constitute basis of scalar Bessel-Gauss beams with a phase singularity of a type of optical vortex located along the optical axis (when $l \neq 0$).

According to Eqs. (6) and (14), the electric fields of arbitrarily homogeneously polarized Gaussian and Bessel-Gauss types of vortex beams with modulating functions Eqs. (17) and (22) are [41]

$$\mathbf{E}_\perp = \text{Re} \left\{ (E_{0x}\mathbf{e}_x + E_{0y}e^{i\phi}\mathbf{e}_y) \times R_t^{|l|} e^{il\varphi} G(\rho, z) e^{i(kz - \omega t)} \right\}, \quad (23)$$

$$\mathbf{E}_\perp^J = \text{Re} \left\{ (E_{0x}\mathbf{e}_x + E_{0y}e^{i\phi}\mathbf{e}_y) \times J_{|l|}(KR_t) Z(\xi) e^{il\varphi} G(\rho, z) e^{i(kz - \omega t)} \right\}, \quad (24)$$

where E_{0x} and E_{0y} are real constant amplitudes of the x - and y -components of the electric field, respectively. By introducing a new constant $\beta = k \sin \alpha$ in Eq. (22) as the angular parameter of the wave vector \mathbf{k} , one can define $K = \beta w_0$, and $Z(\xi) = \exp\{-i\beta^2 z / (2k\xi)\}$. When $l=0$ the Eq. (24) represents the well-known zero order Bessel-Gauss beam [37, 42]. The magnetic field component corresponding to field (24) can be uniquely determined by $c\mathbf{B}_\perp = \mathbf{e}_z \times \mathbf{E}_\perp$.

Following our earlier discussion (see Eqs. 8 and 9), in general, the two-component fields (23) and (24) are vector fields because of different phase factors, $\cos(l\varphi)$ and $\sin(l\varphi)$, in their Cartesian components $\text{Re}\{U_x\} \neq \text{Re}\{U_y\}$. Exception are the beams with zero topological charge $l=0$ and the beams with purely homogeneous linear states of polarization (when $\phi = m\pi$, $m = 0; 1; 2\dots$). They include elliptically polarized fundamental Gaussian and Bessel-Gauss beams (described in the end of the previous section) which are both typical scalar beams. The latter are scalar optical vortex beams as their electric field oscillates in a single direction and they can be described by real part of a single scalar function.

Figures 1 (a) and (b) show examples of the electromagnetic field distribution with function (23) corresponding to the linearly (y -polarized) Gaussian beams with topological charges $l = 1$ and $l = -1$, respectively. The wave fronts of these scalar beams continuously twist such that the field pattern rotates around the beam axis. The pattern contains the zero-field twisted surface which separates the out-of-phase fields. In general, the number of such surfaces corresponds to the topological charge carried by the beam.

As we mentioned above, the fields (23) and (24) represent, in general, elliptically polarized vector beams. Their modulating vector functions (14) admits separation of variables

$$\mathbf{U}(R_t, \varphi, \xi) = f(R_t, \xi) \mathbf{g}(\varphi), \quad (25)$$

with function $\mathbf{g}(\varphi)$

$$\mathbf{g}(\varphi) = (a_x \mathbf{e}_x + a_y e^{i\phi} \mathbf{e}_y) e^{i(l\varphi + \varphi_0)}, \quad (26)$$

and $f = R^{|l|}$ for the Laplace's type, and $f = J_{|l|}(KR_t) Z(\xi)$ for the Helmholtz type of solutions (23), respectively. Let

us look in detail at the particular but interesting case of circularly polarized vortex beams which can be obtained directly from the vector function (26) for $a_x = a_y = \sqrt{2}$ and $\phi = \pm\pi/2$. Then the function (26) becomes

$$\mathbf{g}(\varphi) = e^{i(l\varphi + \varphi_0)} \boldsymbol{\sigma}, \quad (27)$$

where $\boldsymbol{\sigma} = (\mathbf{e}_x + i\sigma\mathbf{e}_y)/\sqrt{2}$ is a unit vector and $\sigma = \pm 1$ with positive (negative) sign corresponding to right (left) hand polarization, and φ_0 is an arbitral initial phase. In the more explicit form, the equation (27) may be represented in the polar basis of radial and azimuthal unit vectors \mathbf{e}_ρ and \mathbf{e}_φ as:

$$\mathbf{g}(\varphi) = (\mathbf{e}_\rho + i\sigma \mathbf{e}_\varphi) \exp\{i[(l + \sigma)\varphi + \varphi_0]\}. \quad (28)$$

Distributions of electric and magnetic fields in vector vortex beams corresponding to the modulating function (28) with $\sigma l = 1$ and $\sigma l = -1$ are shown in Figure 2. One can see that in contrast to scalar case, these vector fields are spatially inhomogeneous and evolve over the period of the fields oscillations. As this spatial evolution depends on both topological charge l and handedness σ , the vector vortex beams carry topology- and polarization-dependent discrete angular momentum along their propagation [43]

$$M_z = (l + \sigma)\hbar. \quad (29)$$

It follows from Eq. (29) that the field rotation around the phase singularity can be decreased or increased by varying circulation of the field vectors at a point.

To conclude this paragraph, let us reiterate the most relevant points. As it clearly seen in Figures 1 and 2 the instantaneous distribution of electromagnetic fields is dramatically different in scalar and vector vortex beams. The field pattern of scalar beams consists of lines of discontinuities in transverse plane at each instant of time. These lines rotate with wave's frequency leading to the time average null intensity along the axis (line of singularity). In contrast, the field pattern of vector beam always possesses a point singularity (null of the field) in its cross-section. This type of discontinuity, which we call a vector singularity, will be discussed in detail in the next Section. As for now, let us note that modulating functions of both vector and scalar vortex beams may not be rigidly coupled in space with the envelope Gaussian wave (5) which serves as a background for topological charges. For clarity we have chosen the specific case of topological charges and the singularity lines located along at the maximum of the Gaussian function (5) (along the beam axis). Generally, the wave field can have many separated topological charges with sufficiently arbitrary trajectories. The singularity lines may extend over three dimensions, and be embedded in the volume filled by the background Gaussian function either forming closed loops or infinite, unbounded lines [44-47].

VECTOR TOPOLOGIES IN PARAXIAL ELECTROMAGNETIC WAVES

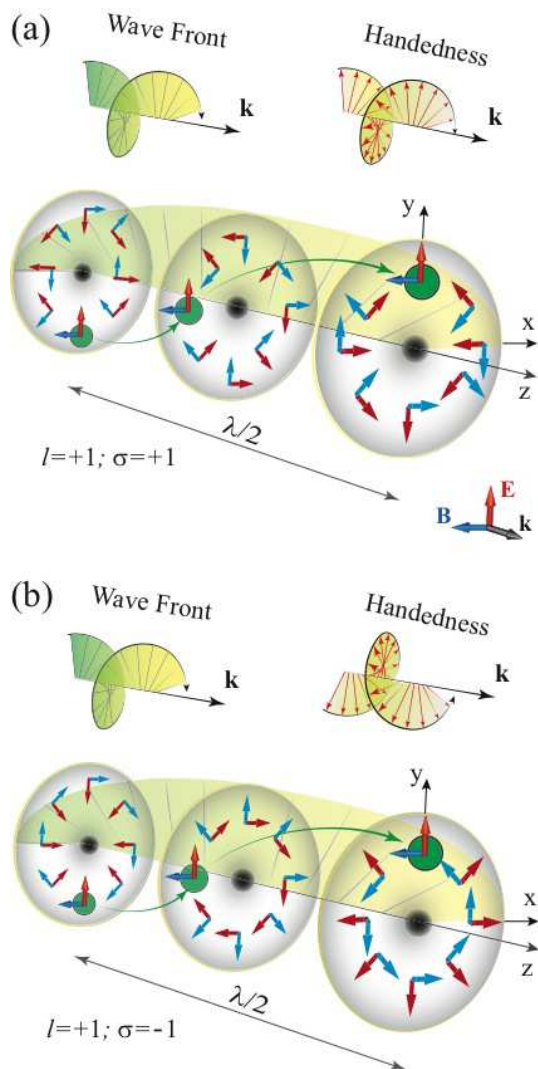


FIG. 2. The instantaneous near-axis distribution of the electromagnetic field in the vector circularly polarized optical vortex with topological charge and handedness a) $l=+1, \sigma=+1$; and b) $l=+1, \sigma=-1$. The evolution of a fixed arbitrary point on the wave surface is shown with green circle.

The singularities essentially change spatial topology of a wave field and, as consequence, the overall intensity pattern. They are the cause of local energy redistributions in the wave beam [19]. However, as the singularities exist only in the host Gaussian envelope (5), they do not influence the general hyperbolic character of the beam self-diffraction. The topological modulating function itself has a physical sense only in combination with the background function which is responsible for the finite energy flux through the cross section of the beam. In other words, the function (5) generates "space" for existence of topological objects in a wave field and it ensures that the spatially unlimited paraxial beam carries a finite power.

When a vortex beam is elliptically polarized, the competition occurs between the phase topology in scalar components of its electromagnetic field and the effect of field orientations due to the wave polarization, as the latter already cannot be ignored [48]. This leads to rich topological patterns of the instantaneous electromagnetic field. The field rotates at every fixed point in space (except the point of singularity) with the wave frequency, while the twisted wave front of the beam rotates with this frequency around a point of the phase singularity (see Fig.2). The result of the both local (at point) and total (in space) rotations is an inhomogeneous distribution of the electromagnetic field in any transverse plane of the vortex beam. Despite the homogeneous state of polarization, the instantaneous field pattern of the beam contains vector singularities as points of an undefined orientation of the fields. In this section, we will discuss these vectorial topological objects which we named instantaneous field (IF) singularities.

Unlike the elliptically polarized vortex beam, the time-averaged pattern of an inhomogeneously distributed field may lead to a nontrivial polarization distribution which may vary in space exhibiting the so-called polarization singularities. These singularities have been considered extensively in the literature [9,25, 26, 49-63]. Here, we will focus on a specific situation when a beam is linearly polarized at any point, but the polarization direction varies azimuthally. In such beams the local rotation of the electric (magnetic) field at a point cancel out the rotation of total field caused by the phase singularity. This mutual cancellation can be achieved through a superposition of waves with opposite topological charges and orthogonal states of polarizations. The idea to use superposition of four uniformly linearly polarized vortex beams to create nonuniformly polarized waves was first proposed by F. Gori [41]. It was further developed, with little variations, to construct more general complex polarization structures [62, 64-70]. Following this technique, we consider the circularly polarized field with modulating functions Eqs. (27), (28). Let us introduce the superposition of these fields having opposite signs of topological charge l and handedness σ , as

$$\mathbf{g}(\varphi) = \sigma^{\pm} e^{i(l\varphi + \varphi_0)} + \sigma^{\mp} e^{-i(l\varphi + \varphi_0)}. \quad (30)$$

The corresponding electric and magnetic fields of Gaussian beams are

$$\begin{aligned}
\mathbf{E}_\perp &= E_0 \text{Re} \left\{ R_t^{|l|} G(\rho, z) e^{i(kz - \omega t)} \right\} \\
&\quad \times (\cos [(l + \sigma)\varphi + \varphi_0] \mathbf{e}_\rho \\
&\quad - \sigma \sin [(l + \sigma)\varphi + \varphi_0] \mathbf{e}_\varphi) \\
\mathbf{B}_\perp &= B_0 \text{Re} \left\{ R_t^{|l|} G(\rho, z) e^{i(kz - \omega t)} \right\} \\
&\quad \times (\sigma \sin [(l + \sigma)\varphi + \varphi_0] \mathbf{e}_\rho \\
&\quad + \cos [(l + \sigma)\varphi + \varphi_0] \mathbf{e}_\varphi),
\end{aligned} \tag{31}$$

where $B_0 = E_0/c$.

The field of vector Bessel-Gauss beams can be found in the similar way

$$\begin{aligned}
\mathbf{E}_\perp^J &= E_0 \text{Re} \left\{ J_{|l|}(KR_t) Z(\xi) G(\rho, z) e^{i(kz - \omega t)} \right\} \\
&\quad \times (\cos [(l + \sigma)\varphi + \varphi_0] \mathbf{e}_\rho \\
&\quad - \sigma \sin [(l + \sigma)\varphi + \varphi_0] \mathbf{e}_\varphi) \\
\mathbf{B}_\perp^J &= B_0 \text{Re} \left\{ J_{|l|}(KR_t) Z(\xi) G(\rho, z) e^{i(kz - \omega t)} \right\} \\
&\quad \times (\sigma \sin [(l + \sigma)\varphi + \varphi_0] \mathbf{e}_\rho \\
&\quad + \cos [(l + \sigma)\varphi + \varphi_0] \mathbf{e}_\varphi).
\end{aligned} \tag{32}$$

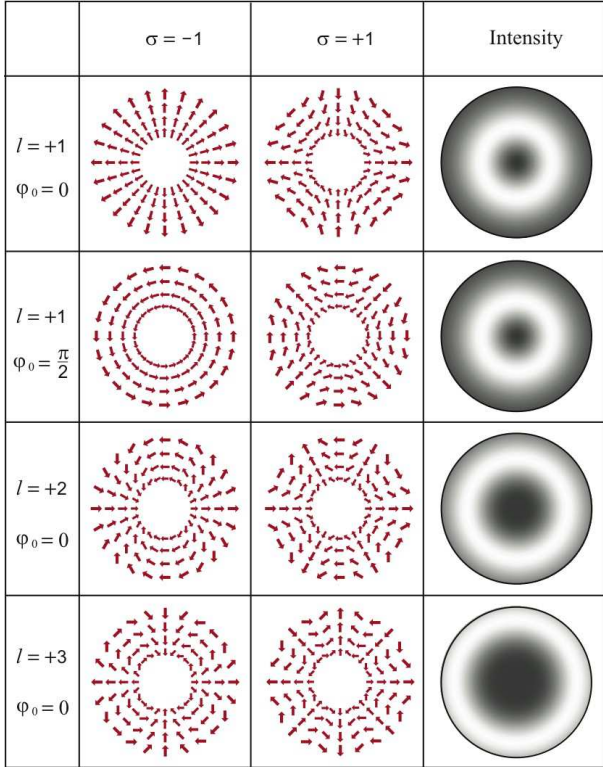


FIG. 3. Examples of electric field distribution (second and third columns) and intensity (fourth column) of vector beams described by Eq. (31). Only the intensity of x-polarized component of the beams is shown.

Both Eq.(31) and Eq.(32) types of beams possess similar topological properties. Hence, without loss of generality, we will concentrate below on the Gaussian beams ex-

pressed by Eq.(31). Figure 3 depicts few examples of electric field distribution in such beams. These patterns correspond to pure linear states of polarization at any point of a transverse plane, but the direction of the polarization depends on the azimuthal position. The angular and spin momenta of the beams are zero and, consequently, the numbers l and σ in Eqs.(31, 32) can no longer be interpreted as topological charge and spin, respectively. Nevertheless, these numbers have a new meaning as indices within the symmetry group in the beams. The group with the same index l splits into two subgroups according to σ . These subgroups $l\sigma$ have own symmetry with unique distribution of the electric (magnetic) field and cannot be transformed from one to another without symmetry breaking. Each subgroup $l\sigma > 0$ or $l\sigma < 0$ with a fixed l permits local rotations of fields by the same angle at every point of the wave front by changing initial phase φ_0 . The local rotations by the angle φ_0 are equal to a total rotation of the electric (magnetic) field pattern by the angle $\varphi_0/2$ around the beam center preserving field symmetry in every subgroup except $l\sigma = -1$ (see Fig. 3). Despite the absence of topological charges in the vector beams Eqs.(31),(32), the field configuration still carries IF singularities originating from the undefined direction of the *instantaneous* field vectors. They may have a source, spiral, sink, saddle or circulation morphology as shown in Figure 3. In particular case described in this Section, the IF singularities are isolated points at the axis $\rho=0$ in a beam transverse plane. Their position and time-average morphology coincide with vector point singularities (V -points) proposed by I. Freund as points at which the orientation the electric (magnetic) vectors of a linearly polarized field becomes undefined [52]. However, there are significant differences between them. The V -points are singularities in the state of polarization rather than fields and, thus, as it was embraced by I. Freund, they always belong to linearly polarized waves. In contrast, the IF singularities may exist in any state of polarization. The example is the singularities in circularly polarized optical vortices shown in Section 2 (see Fig. 2 and the text below). Their electric (magnetic) fields contain IF singularities at every moment of time (see Fig. 3). Another difference is generally nonstationary behaviour of the IF singularities, as we will show in the next Section. Thus, the vector field singularities are pure property of instantaneous field configuration. From the Eq. (32), one can see that in the vicinity of IF singularities

$$\begin{aligned}
\oint \mathbf{E}_\rho \mathbf{n} dl &= c \oint \mathbf{B}_\varphi dl \\
c \oint \mathbf{B}_\rho \mathbf{n} dl &= - \oint \mathbf{E}_\varphi dl,
\end{aligned} \tag{33}$$

where \mathbf{n} is the unit vector normal to the infinitesimal element of the loop dl . The line integral of fields is calculated over the closed equiphase loop coinciding with a circle of equal intensity in the beam transverse section.

These integrals are equal to zero for any subgroups except for $l\sigma=-1$ because \mathbf{g}_ρ and \mathbf{g}_φ components of vector function

$$\mathbf{g}(\varphi) = \cos[(l+\sigma)\varphi + \varphi_0] \mathbf{e}_\rho - \sigma \sin[(l+\sigma)\varphi + \varphi_0] \mathbf{e}_\varphi \quad (34)$$

change sign $2(l+\sigma)$ times along the closed loop. Nominally, such field configuration is similar to two-dimensional vector fields of $N=2|l+\sigma|$ charge “sources” (or currents) symmetrically localized in the vicinity of the axis $\rho=0$ for the $l\sigma<0$ and at infinity $\rho \rightarrow \infty$ for $l\sigma>0$. The parity of these sources leads to cancellation of the loop integrals Eq.(33) in the vicinity of the IF singularity.

The exceptional subgroup $l\sigma=-1$ is unique as the vector field \mathbf{g} retains fixed orientation along the loop. This corresponds to a spirally oriented vector field \mathbf{g} with two extreme cases $\varphi=0$ and $\varphi=\pi/2$ of pure radial and azimuthal orientations when the function (34) is independent of the coordinate φ

$$\mathbf{g} = \mathbf{e}_\rho, \quad \text{when } \varphi_0 = 0, \quad (35)$$

and

$$\mathbf{g} = \mathbf{e}_\varphi, \quad \text{when } \varphi_0 = \pi/2. \quad (36)$$

Electric fields associated with these modulating functions correspond to axially symmetric, radially and azimuthally polarized beams, respectively, known in optics as TM and TE beams (see [27] and references therein). The electromagnetic field of the TM and TE beams are

$$\begin{aligned} \mathbf{E}_\perp^{TM} &= E_0 \text{Re} \{ f(R_t, \xi) G e^{i(kz-\omega t)} \} \mathbf{e}_\rho \\ \mathbf{B}_\perp^{TM} &= B_0 \text{Re} \{ f(R_t, \xi) G e^{i(kz-\omega t)} \} \mathbf{e}_\varphi, \end{aligned} \quad (37)$$

and

$$\begin{aligned} \mathbf{E}_\perp^{TE} &= E_0 \text{Re} \{ f(R_t, \xi) G e^{i(kz-\omega t)} \} \mathbf{e}_\varphi \\ \mathbf{B}_\perp^{TE} &= -B_0 \text{Re} \{ f(R_t, \xi) G e^{i(kz-\omega t)} \} \mathbf{e}_\rho. \end{aligned} \quad (38)$$

As it is clearly seen, the field pattern has uncompensated instantaneous radial component of electric (for the TM) and magnetic (for the TE) field on any closed circular loop in the beam transverse section. Such pattern corresponds to intriguing field configurations (see Fig. 4) as the integrals in Eq. 33 are not equal to zero on the loop. Formally, according to the integral form of Maxwell's equations, this means existence of uncompensated charges (monopoles) and their currents in the vicinity of the IF singularity. To demonstrate this, let us consider the fields (37) and (38) at the plane $z=0$ near the point $R_t=0$. Taking into account that $f=R_t$ and using the first-order Taylor series approximation of the field functions near the axis $\rho=0$, the both (37) and (38) fields approximately are:

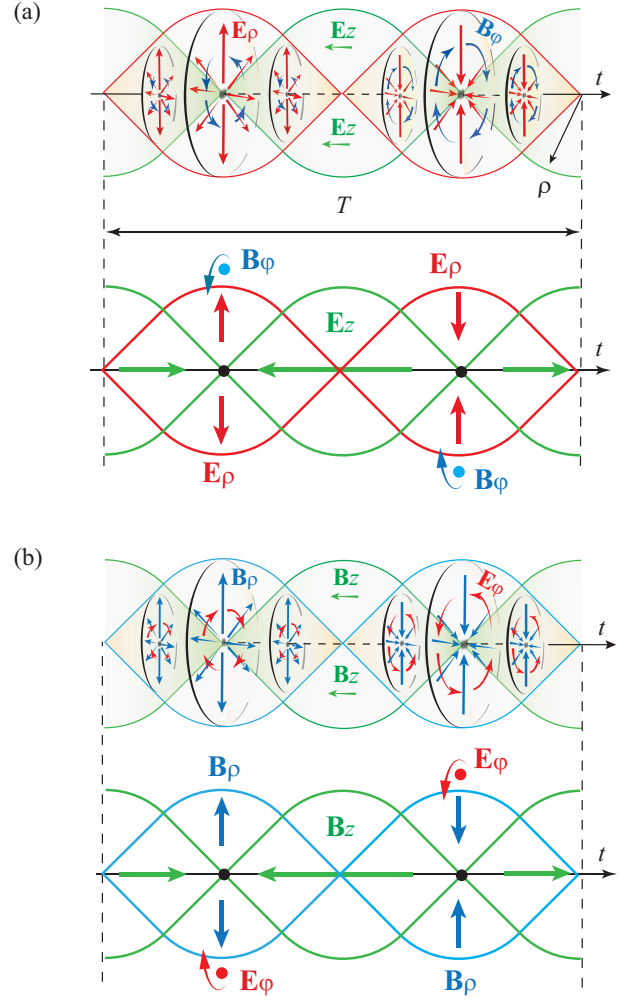


FIG. 4. Field distributions over the wave period of the radially (a) and azimuthally (b) polarized vector beams. Instantaneous field singularities manifest themselves as virtual sources and sinks of a vector fields in points of zero field amplitude. Each source/sink of the transverse field is, at the same time, a sink/source of the longitudinal component of the field.

$$\mathbf{E}_\perp^{TM} \approx E_0 R_t \cos \omega t \mathbf{e}_\rho \quad (39)$$

$$\mathbf{B}_\perp^{TM} \approx B_0 R_t \cos \omega t \mathbf{e}_\varphi,$$

and

$$\mathbf{E}_\perp^{TE} \approx E_0 R_t \cos \omega t \mathbf{e}_\varphi \quad (40)$$

$$\mathbf{B}_\perp^{TE} \approx -B_0 R_t \cos \omega t \mathbf{e}_\rho.$$

Consider a closed circular loop of equal field amplitudes in the $z=0$ plane with the centre at a point $\rho=0$ and a radius R as shown in Fig.5. Let $\mathbf{l} = \mathbf{e}_\varphi$ be a unit vector along the loop and $\mathbf{n} = \mathbf{e}_\rho$ be a unit vector normal to the infinitesimal element dl of the loop. Then the electric

and magnetic field fluxes in radial direction through the loop, for $R \rightarrow 0$, are

$$\lim_{\Delta S \rightarrow 0} \frac{\oint \mathbf{E}^{TM} \mathbf{n} dl}{\Delta S} \approx (2E_0/w_0) \cos \omega t \quad (41)$$

$$\lim_{\Delta S \rightarrow 0} \frac{\oint \mathbf{B}_\perp^{TE} \mathbf{n} dl}{\Delta S} \approx - (2B_0/w_0) \cos \omega t,$$

where we used the fact that the loop length $\oint dl = 2\pi R$ and area, $\Delta S = \pi R^2$. On the other hand, as the electric (magnetic) field flows through the closed loop, the dual to it magnetic (electric) field circulates around the loop:

$$\lim_{\Delta S \rightarrow 0} \frac{\oint \mathbf{B}_\perp^{TM} dl}{\Delta S} \approx (2B_0/w_0) \cos \omega t \quad (42)$$

$$\lim_{\Delta S \rightarrow 0} \frac{\oint \mathbf{E}_\perp^{TE} dl}{\Delta S} \approx (2E_0/w_0) \cos \omega t.$$

The expressions (41) can be converted into the field fluxes through the closed infinitesimal cylindrical surface Ω with the length $c\Delta t$ along the z direction and the volume $\Delta V = c\Delta t \Delta S$ in the time interval $t + \Delta t$, as:

$$\begin{aligned} \oint \mathbf{E}_\perp^{TM} \mathbf{n} d\Omega &= c \int_t^{t+\Delta t} \oint \mathbf{E}_\perp^{TM} \mathbf{n} dl dt \\ &\approx 2\pi c R^2 (E_0/w_0) \int_t^{t+\Delta t} \cos \omega t dt \\ &= 2\pi c R^2 (E_0/\omega w_0) [\sin(\omega(t + \Delta t)) - \sin(\omega t)] \\ \oint \mathbf{B}_\perp^{TE} \mathbf{n} d\Omega &= c \int_t^{t+\Delta t} \oint \mathbf{B}_\perp^{TE} \mathbf{n} dl dt \\ &\approx -2\pi c R^2 (B_0/w_0) \int_t^{t+\Delta t} \cos \omega t dt \\ &= 2\pi c R^2 (B_0/\omega w_0) [\sin(\omega t) - \sin(\omega(t + \Delta t))] \end{aligned} \quad (43)$$

We may assume that Δt is very small such that the time variation of fields is nearly uniform over the cylindrical area. Then the electric and magnetic fluxes through the closed cylindrical surface divided by the volume ΔV are given by

$$\begin{aligned} \lim_{\Delta V \rightarrow 0} \frac{\oint \mathbf{E}_\perp^{TM} \mathbf{n} d\Omega}{\Delta V} &\approx (2E_0\omega\Delta t/w_0) \cos \omega t \\ \lim_{\Delta V \rightarrow 0} \frac{\oint \mathbf{B}_\perp^{TE} \mathbf{n} d\Omega}{\Delta V} &\approx - (2B_0\omega\Delta t/w_0) \cos \omega t \end{aligned} \quad (44)$$

Formally, according to Eqs.(42) and (44), the IF singularities Eq.(35) and Eq.(36), are source of non-compensated fluxes and circulations of the transverse fields through the side area of the cylindrical surface. This is why we named corresponding IF singularities as topological monopoles and currents. The field oscillations periodically change signs of the fluxes Eq.(44) and circulations Eq.(42) in any fixed plane section $z = \text{const}$ leading to zero average values over the wave period T , as it shown in the Fig.4. These fluxes and circulations remain finite with the same

signs between two zero points on a half period $T/2$ of oscillations (or on a half wavelength distance along z -axis).

Note, that this flux anomaly appearing in the transverse components of the wave field is removed by including the longitudinal field components as their fluxes through the closed surface (here through bases of the cylindrical surface) exactly compensate the fluxes of the transverse fields. Although in the zero-order paraxial approximation the longitudinal z -components of electric and magnetic fields are ignored, they appear in the next, first-order paraxial approximation as $\omega F_z = i c \nabla_\perp F_\perp$ [27]. As an example, let us consider the longitudinal field flux through the plane $z=0$ in the radially polarized beam of Eq. 39. In such a beam the electric field with the complex function $F_z = 2icE_0/\omega w_0$ represents the amplitude of longitudinal field, and is defined by Eqs.(37) and (39) as:

$$E_z = 2E_0 \sin(\omega t)/kw_0 \quad (45)$$

The longitudinal field Eq. (45) is out of phase with respect to the transverse components Eq. (39) and its orientation is shown in the Fig. 4. The resulting electric field flux of the longitudinal field through the cylindrical bases ΔS is

$$\begin{aligned} \oint \mathbf{E}_z^{TM} \mathbf{n} d\Omega &= \\ &= -2\pi c R^2 (E_0/\omega w_0) [\sin(\omega(t + \Delta t)) - \sin(\omega t)], \end{aligned} \quad (46)$$

and exactly cancels the flux of the transverse components of the electromagnetic field depicted by Eq. (43) .

Figure 5 schematically shows fluxes and circulations of electric \mathbf{E} and magnetic \mathbf{B} fields on the cylindrical surface around the beams axes with the length of side equal to a fraction of wavelength $\Delta\lambda$.

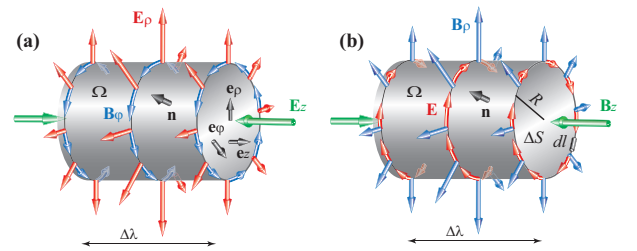


FIG. 5. Fluxes and circulations of the electric \mathbf{E}_\perp and magnetic \mathbf{B}_\perp field at the fraction of wavelength $\Delta\lambda$ in radially (a) and azimuthally (b) polarized vector beams. In the radially (azimuthally) polarized beam, the transverse field \mathbf{E}_ρ (\mathbf{B}_ρ) has nonzero flux through the side area of a closed cylindrical surface Ω , while the field \mathbf{B}_ϕ (\mathbf{E}_ϕ) circulates around the closed loop on the surface. The flux of the longitudinal field \mathbf{E}_z (\mathbf{B}_z) through the bases S of radius R compensates the transverse flux. The axis of the cylinder coincides with the beam axis.

The aforementioned topological monopoles, as well as the other IF singularities of electromagnetic waves, are caused solely by the spatial configuration of the surrounding transverse vector fields. However, the full electromagnetic field of vector beams remains regular as all vector fields acquire physical values everywhere in the beams except the zero-field singular point.

POLARIZATION TOPOLOGY VIA MOVING IF SINGULARITIES

All considerations on instantaneous vector singularities in the previous section refer to vector beams with a uniform state of polarization inhomogeneously distributed in space. In general, both orientation of the field vectors and ellipticity of the polarization can vary from point to point. In three dimensions, when the state of elliptic polarization changes with position, points of circular polarization appear along the so called C-lines, while the states of linear polarization with undetermined handedness define L-surfaces [25, 26, 52, 56]. In the transverse cross-section, a L-surface is represented by the line. This line is swept out by at least one moving isolated singularity where *instantaneous* electric and magnetic fields are zero, and their directions are therefore undetermined. These singularities were first described by J. Nye and were originally named as “wave disclinations” [25]. Later, M. Dennis called them “relative singularities” because their instantaneous position is phase-dependent [56].

The difference between the IF singularities in uniformly polarized beams, described above, and wave disclinations in beams with variant state of polarization is their dynamics. The IF singularities may have a stable spatial position and exist even in a wave with homogeneous state of polarization, while wave disclinations change their location in space over time sweeping out a L-surface. Although the instantaneous value of the electric (magnetic) field is equal to zero at points of wave disclinations, the field averaged over a period of wave oscillations has a nonzero value. This time-averaged field imprints a nonzero intensity on the L-surface on which the polarization becomes linear. As this is only a difference in the averaged picture, the wave disclinations are a particular case of IF singularities in our terminology. The morphology of a moving wave disclination belongs to the group $l\sigma = \pm 1$ of IF singularities and may be of source, spiral, sink, circulation or saddle morphology (see Fig. 3). The subgroup $l\sigma = -1$ contains wave monopoles and currents of an instantaneous electromagnetic field in vicinity of singular points, similar as it did in the stationary case.

The dynamic behaviour of the IF singularities affects the time-averaged polarization states leading to polarization singularities - places related to C-lines and L-surfaces in beams with variation of state of polarization. Because

of their average nature, polarization singularities are not equal to the IF singularities and may even appear in points different from that of IF singularities. The dynamics of vector singularities can be simply illustrated through superposition of scalar and vector beams shown in previous Sections, as it leads to beams with typical polarization singularities. More precisely, we combine m vector modulating functions (25) and (28) with arbitral topological charges l_n and handedness σ_n

$$\mathbf{U} = \sum_{n=1}^m A_n (\mathbf{e}_\rho + i\sigma_n \mathbf{e}_\varphi) f_n \exp(i(l_n + \sigma_n)\varphi), \quad (47)$$

where A_n is arbitrary constant. For simplicity, we ignore initial phase in each function.

The simplest superposition of the type (47) with non-trivial vector topology is sum of just two terms. The first term is a non-singular modulation function with the topological charge $l_1 = 0$ and handedness $\sigma_1 = -1, +1$. The second term is a function with topological charge $l_2 = -1, +1$ and handedness $\sigma_2 = -1, +1$, which corresponds to a circularly polarised single charge vortex beam. The superposition of functions with the same handedness $\sigma_1 \times \sigma_2 = 1$ leads to the case of homogeneously circularly polarized vortex beams considered in the previous Section. The difference is only the position of a singularity, which now is out of the optical axis. The other pair with opposite signs of handedness $\sigma_1 \times \sigma_2 = -1$ gives us vector beams with the following modulation functions

$$\begin{aligned} \mathbf{U}_{11} = & A_1(\mathbf{e}_\rho + i\mathbf{e}_\varphi) \exp(i\varphi) f_1 \\ & + A_2(\mathbf{e}_\rho - i\mathbf{e}_\varphi) f_2, \end{aligned} \quad (48)$$

$$\begin{aligned} \mathbf{U}_{12} = & A_1(\mathbf{e}_\rho - i\mathbf{e}_\varphi) \exp(-i\varphi) f_1 \\ & + A_2(\mathbf{e}_\rho + i\mathbf{e}_\varphi) f_2 \exp(2i\varphi), \end{aligned}$$

and

$$\begin{aligned} \mathbf{U}_{21} = & A_1(\mathbf{e}_\rho - i\mathbf{e}_\varphi) \exp(-i\varphi) f_1 \\ & + A_2(\mathbf{e}_\rho + i\mathbf{e}_\varphi) f_2, \end{aligned} \quad (49)$$

$$\begin{aligned} \mathbf{U}_{22} = & A_1(\mathbf{e}_\rho + i\mathbf{e}_\varphi) \exp(i\varphi) f_1 \\ & + A_2(\mathbf{e}_\rho - i\mathbf{e}_\varphi) f_2 \exp(-2i\varphi). \end{aligned}$$

The pairs $(\mathbf{U}_{11}, \mathbf{U}_{12})$ and $(\mathbf{U}_{21}, \mathbf{U}_{22})$ represent functions with opposite chiralities and can be transformed into each other via mirror reflection: $\sigma \rightarrow -\sigma$; $l \rightarrow -l$. Hence, it is sufficiently to consider only the field (48). Vector beams represented by this superposition are named Poincaré beams because their polarization states cover entire surface of the Poincaré sphere [71-75]. If we choose the functions $f_n = R_t^{|l_n|}$, then the electric fields of both beams are

$$\mathbf{E}_1 = \text{Re} [E_{01}(\mathbf{e}_\rho + i\mathbf{e}_\varphi) \exp(i\varphi) + E_{02}R_t(\mathbf{e}_\rho - i\mathbf{e}_\varphi)]G(\rho, z)e^{i(kz-\omega t)} \quad (50)$$

$$\mathbf{E}_2 = \text{Re} [E_{01}(\mathbf{e}_\rho - i\mathbf{e}_\varphi) \exp(-i\varphi) + E_{02}R_t(\mathbf{e}_\rho + i\mathbf{e}_\varphi) \exp(2i\varphi)]G(\rho, z)e^{i(kz-\omega t)},$$

where E_{0n} are arbitrary amplitude constants. The Bessel-Gauss type of Poincaré beams can be obtained in a similar way by taking $f = J_{|l_n|}(KR_t)Z(\xi)$.

The electric field evolution of the beams given by Eqs. (50) is depicted in Fig. 6 (a, b). At any moment of time, the isolated point of the IF singularity lies on a L-line in the transverse plane of the beams. This point rotates completing a full circle along the L-line during a half period of field's oscillations. At the same time the IF singularity experiences a periodic transformation of its structure (see the bottom panels in Fig. 6) similar to that of stationary IF singularities in circularly polarized vortex beams (see Fig.2).

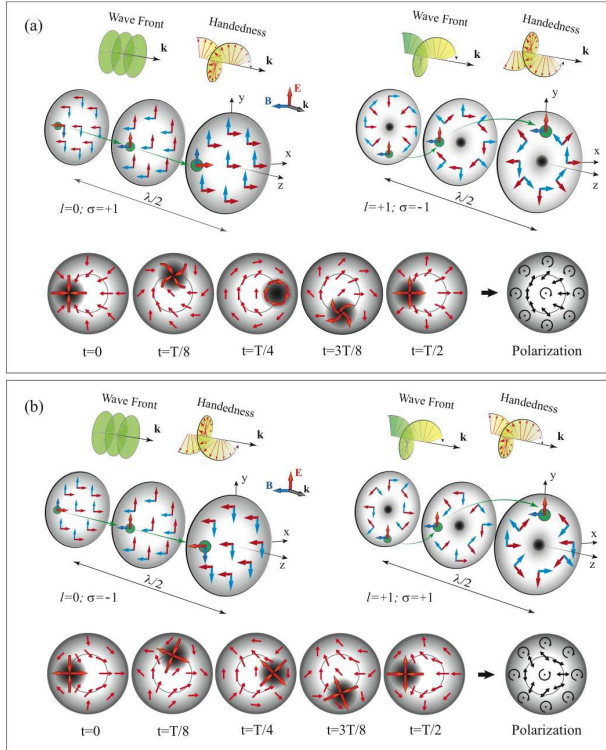


FIG. 6. Field distribution and its dynamics in superposition [Eq.(48)] of circularly polarized Gaussian (left graph) and vortex beams (right graph) when a) $l_1=0; \sigma_1=1; l_2=1; \sigma_2=-1$, and b) $l_1=0; \sigma_1=-1; l_2=1; \sigma_2=+1$. The evolution of a fixed arbitrary point on the wave surface is shown with a green circle. The bottom row in (a) and (b) panels depicts the snapshots of electric component of the field taken in few time instants, as well as the resulting polarization structure of the beam.

In three dimensions the distribution of the instantaneous field of Poincaré beams (50) with a single topolog-

ical charge contains a single line of IF singularity where the field is discontinuous. This line sweeps out the L-surface with the field oscillation as the IF singularity rotates with double wave frequency around the beam axis while the axis becomes a C-line with the circular state of polarization. As topological charge of Poincaré beams (50) is uncompensated, these beams carry orbital angular momentum and the whole polarization pattern rotates in propagation.

It is worth to note that unlike L-surfaces, C-lines are free from physical discontinuities of electromagnetic fields and have no IF singularities. The C-lines result from dynamic behaviour of the IF singularities on the L-surface. The topology of the polarization patterns in the vicinity of the C-point (transverse section of the C line) is related to average field orientations rather than to the field discontinuous. Those patterns are typically named as “lemon”, “star” and “monstar” [56, 77]. Classification of C-points constitutes an extended topic discussed extensively in the literature (see for instance [49-56, 77-79] and review [9]). As they do not possess the IF singularities, which are our main interest here, we only remark that Poincaré beams given by Eqs.(50) and demonstrated in Fig.6 (a), and (b), contain a “star” and a “lemon” C-points, respectively.

In closing of this Section let us note that we have chosen one of the simplest possible superposition of modulating functions (28) to clarify the instantaneous field singularities on polarization singularities. The selected superposition of the scalar function (corresponding to circularly polarized Gaussian beam) and the vector function (corresponding to circularly polarized vortex beam) is not the only one covering all states of polarization and leading to polarization singularities. The other simplest type of Poincaré beams can be constructed by the following superposition [80]

$$\mathbf{U} = A_1\mathbf{e}_x + A_2R_t\mathbf{e}_y \exp(\pm i\varphi). \quad (51)$$

Each of the constituent functions is a scalar by itself as it represents a single Cartesian component, but their superposition is a fully vectorial function (see Eq.(9)).

CONCLUSIONS

We presented here systematic description of topological singularities in both electric and magnetic field of the electromagnetic waves, in a paraxial approximation. In particular, we emphasized the basic physical principles underlying the role of instantaneous singularities. It appears that singularities essentially define a spatial topology of the surrounding wave field but not the evolution of wave packet in space and hence these two aspects can be analyzed separately. The envelope function generates scalar “wave space” for the existence of phase, polarization or instantaneous vector field singularities defining

the finite energy flux of electromagnetic field. The representation of the singularities by a single abstract modulating function greatly simplifies their formal description and, consequently, understanding of their fundamental nature.

The undefined direction of electromagnetic field vectors at points of singularities leads to paradoxical effect – the instantaneous spatial distributions of the transverse field components around the singularities appear as if they were originating from 2D “virtual” electric or magnetic sources. These apparent topological monopoles are result of the particular spatial configuration of the transverse components of the electromagnetic field.

ACKNOWLEDGMENT

The authors acknowledge the support from the Australian Research Council and the Qatar National Research Fund (grant NPRP8-246-1-060). We also thank the Anonymous Referee who helped us to significantly improve our work.

-
- [1] M. Born, and E. Wolf, *Principles of Optics* (Pergamon Press, Oxford, 1980).
- [2] D. S. Jones, *The Theory of Electromagnetism* (Pergamon Press, New York, 1964).
- [3] B. Polat, *Remarks on the fundamental postulates on field singularities in electromagnetic theory*, IEEE Antennas Propag. Mag. **47**, 47 (2005).
- [4] J. F. Nye and M. V. Berry, *Dislocations in wave trains*, Proc. R Soc. Lond. A **336**, 165 (1974).
- [5] L. Allen, M.J. Padgett, and M. Babiker, *Orbital angular momentum of light*, Prog. Opt. **39**, 291 (1999).
- [6] M.S. Soskin and M.V. Vasnetsov, *Singular optics*, Prog. Opt. **42**, 219 (2001).
- [7] S. Franke-Arnold, L. Allen, and M. J. Padgett, *Advances in optical angular momentum*, Laser & Photon. Rev. **2**, 299 (2008).
- [8] A. Bekshaev, M. Soskin and M. Vasnetsov, *Paraxial Light Beams with Angular Momentum* (Nova Science Publishers, New York, 2008).
- [9] M. R. Dennis, K. O’Holleran, and M. J. Padgett, *Singular Optics: Optical Vortices and Polarization Singularities*, Prog. Opt. **53**, 293 (2009).
- [10] M. Soskin, S. V. Boriskina, Y. Chong, M. R. Dennis, A. Desyatnikov, *Singular optics and topological photonics*, J. Opt. **19**, 010401 (2016).
- [11] H. Kogelnik and T. Li, *Laser beams and resonators*, Appl. Opt. **5**, 1550 (1966).
- [12] A. Yariv, *Quantum Electronics* (Wiley, 1989).
- [13] A. E. Siegman, *Lasers* (University Science Books, 1986).
- [14] M. Berry, *Making waves in physics*, Nature **403**, 21 (2000).
- [15] G. A. Swartzlander, *Optical vortices* (CRC Press, 2014).
- [16] M. J. Padgett, L. Allen, *The Poynting vector in Laguerre-Gaussian laser modes*, Opt. Commun. **121**, 36 (1995).
- [17] L. Allen, S. M. Barnett and M. J. Padgett (eds.) *Optical Angular Momentum* (Taylor and Francis, London 2003).
- [18] Andrews D L and Babiker M (ed.), *The Angular Momentum of Light* (Cambridge: Cambridge University Press, 2012).
- [19] A. Bekshaev, K. Y. Bliokh and M. Soskin, *Internal flows and energy circulation in light beams*, J. Opt. **13**, 053001 (2011).
- [20] G. Molina-Terriza, J.P. Torres and L. Torner, *Twisted photons*, Nat. Phys. **3**, 305 (2007).
- [21] L. Marrucci, et al., *Spin to orbital conversion of the angular momentum of light and its classical and quantum applications*, J. Opt. **13**, 064001 (2011).
- [22] K. Y. Bliokh, Y. P. Bliokh, S. Savelev, and F. Nori, *Semi-classical dynamics of electron wave packet states with phase vortices*, Phys. Rev. Lett. **99**, 190404 (2007).
- [23] J. Verbeeck, H. Tian, and P. Schattschneider, Nature **467**, 301 (2010).
- [24] R. Shiloh, Y. Tsur, R. Remez, Y. Lereah, B. A. Malomed, V. Shvedov, C. Hnatovsky, W. Krolikowski, A. Arie, *Unveiling the orbital angular momentum and acceleration of electron beams*, Phys. Rev. Lett. **114**, 096102 (2015).
- [25] J. F. Nye, *Polarization effects in the diffraction of electromagnetic waves: the role of disclinations*, Proc. R Soc. Lond. A **387**, 105 (1983).
- [26] J.F. Nye, *Lines of circular polarization in electromagnetic wave fields*, Proc. R Soc. Lond. A **389**, 279 (1983).
- [27] M. Lax, W. Louisell and W.B. Mcknight, *From Maxwell to paraxial wave optics*, Phys. Rev. A **11**, 1365 (1975).
- [28] W. Jr. Miller, *Symmetry and Separation of Variables* (Addison-Wesley, 1977).
- [29] J. C. Gutierrez-Vega and M. A. Bandres, *Helmholtz-Gauss waves*, J. Opt. Soc. Am. A **22**, 289 (2005).
- [30] M. A. Bandres and J. C. Gutierrez-Vega, *Vector Helmholtz-Gauss and vector Laplace-Gauss beams*, Opt. Lett. **30**, 2155 (2005).
- [31] M. A. Bandres and J. C. Gutierrez-Vega, *Ince-Gaussian beams* Opt. Lett. **29**, 144 (2004).
- [32] M. A. Bandres, *Elegant Ince?Gaussian beams*, Opt. Lett. **29**, 1724 (2004).
- [33] E. G. Abramochkin and V. G. Volostnikov, *Generalized Gaussian beams*, J. Opt. A, Pure Appl. Opt. **6**, S157 (2004).
- [34] M. A. Bandres and J. C. Gutierrez-Vega, *Vector Helmholtz-Gauss and vector Laplace-Gauss beams*, Opt. Lett. **30**, 2155–2157 (2005).
- [35] E. Karimi, G. Zito, B. Piccirillo, L. Marrucci, E. Santamato, *Hypergeometric-Gaussian modes*, Opt. Lett. **29**, 3053 (2007).
- [36] V. V. Kotlyar, R. V. Skidanov, S. N. Khonina, V. A. Soifer, *Hypergeometric modes*, Opt. Lett. **32**, 742 (2007).
- [37] D. G. Hall, *Vector-beam solutions of Maxwell’s wave equation*, Opt. Lett. **21**, 9 (1996).
- [38] A. P. Kiselev, *New structures in paraxial Gaussian beams*, Opt. Spectrosc. **96**, 533 (2004).
- [39] S. Axler, P. Bourdon, W. Ramey, *Harmonic Function Theory* (Springer, New York, 2001).
- [40] V. Shvedov, C. Hnatovsky, N. Shostka, W. Krolikowski, *Generation of vector bottle beams with a uniaxial crystal*, J. Opt. Soc. Am. B **30**, 1 (2013).
- [41] F. Gori, *Polarization basis for vortex beams*, J. Opt. Soc. Am. A **18**, 1612 (2001).
- [42] F. Gori, G. Guattari, *Bessel-Gauss beams*, Opt. Comm. **64**, 491 (1987).

- [43] A. M. Yao and M. J. Padgett, *Orbital angular momentum: origins, behavior and applications*, Adv. Opt. Photonics **3**, 161 (2011).
- [44] K. O'Holleran, M. R. Dennis and M. J. Padgett, *Topology of light's darkness*, Phys. Rev. Lett. **102**, 143902 (2009).
- [45] M. R. Dennis, R. P. King, B. Jack, K. O'Holleran, M. J. Padgett, *Isolated optical vortex knots*, Nat. Phys. **6**, 118 (2010).
- [46] D. Kleckner and W. Irvine, *Creation and dynamics of knotted vortices* Nat. Phys. **9** 253–258 (2013).
- [47] H. Kedia, I. Bialynicki-Birula, D. Peralta-Salas, W. T. M. Irvine, *Tying Knots in Light Fields*, Phys. Rev. Lett. **111**, 150404 (2013).
- [48] K. Y. Bliokh, F. J. Rodriguez-Fortuo, F. Nori, A. V. Zayats, *Spin-orbit interactions of light*, Nat. Photon. **9**, 796–808 (2015).
- [49] J. F. Nye and J. V. Hajnal, *The wave structure of monochromatic electromagnetic radiation*, Proc. R. Soc. Lond. A Math. Phys. Sci. **409**, 21 (1987).
- [50] J. V. Hajnal, *Singularities in the transverse field of electromagnetic waves. I Theory*, Proc. R. Soc. Lond. A Math. Phys. Sci. **414**, 433 (1987).
- [51] I. Freund, *Polarization flowers*, Opt. Commun. **199**, 47 (2001).
- [52] I. Freund, *Polarization singularity indices in Gaussian laser beams*, Opt. Commun. **201**, 251–270 (2002).
- [53] I. Freund, M. S. Soskin, and A. I. Mokhun, *Elliptical critical points in paraxial optical fields*, Opt. Commun. **208** (4-6), 223–253 (2002).
- [54] I. Freund, A. I. Mokhun, M. S. Soskin, O. V. Angelsky, and I. I. Mokhun, *Stokes singularity relations*, Opt. Lett. **27** (7), 545–547 (2002).
- [55] A. I. Mokhun, M. S. Soskin, and I. Freund, *Elliptical critical points: C-points, a-lines, and the sign rule*, Opt. Lett. **27** (12), 995–997 (2002).
- [56] M. R. Dennis, *Polarization singularities in paraxial vector fields: morphology and statics*, Opt. Commun. **213**, 201–221 (2002).
- [57] T. H. Lu, Y. F. Chen, and K. F. Huang, *Generalized hyperboloid structures of polarization singularities in Laguerre-Gaussian vector fields*, Phys. Rev. A **76**, 063809 (2007).
- [58] C. Hnatovsky, V. Shvedov, W. Krolikowski, A. Rode, *Revealing local field structure of focused ultrashort pulses*, Phys. Rev. Lett. **106**, 123901 (2011).
- [59] I. Freund, *Ordinary polarization singularities in three-dimensional optical fields*, Opt. Lett. **37**, 2223 (2012).
- [60] I. Freund, *Mbius strip and twisted ribbon in intersecting Gauss-Laguerre beams*, Opt. Commun. **284**, 3816 (2011).
- [61] V. Kumar and N. K. Viswanathan, *Topological structures in vector-vortex beam fields*, J. Opt. Soc. Am. B **31**, A40 (2014).
- [62] B. Khajavi and E. Galvez, *High-order disclinations in space-variant polarization*, J. Opt. **18**, 084003 (2016).
- [63] Zhan Q, *Cylindrical vector beams: from mathematical concepts to applications*, Advances in Optics and Photonics **1**, 1 (2009).
- [64] A. A. Tovar, *Production and propagation of cylindrically polarized Laguerre-Gaussian laser beams*, J. Opt. Soc. Am. A **15**, 2705 (1998).
- [65] C. F. Li, *Integral transformation solution of free-space cylindrical vector beams and prediction of modified Bessel-Gaussian vector beams*, Opt. Lett. **32**, 3543 (2007).
- [66] P. Senthilkumaran, J. Masajada, and S. Sato, *Interferometry with vortices*, Int. J. Opt. **2012**, 517591 (2012).
- [67] S. Vyas, Y. Kozawa, and S. Sato, *Polarization singularities in superposition of vector beams*, Opt. Express **21**, 8972 (2013).
- [68] T. Ando, N. Matsumoto, Y. Ohtake, Yu. Takiguchi, and T. Inoue, *Structure of optical singularities in coaxial superposition of Laguerre-Gaussian mode*, J. Opt. Soc. Am. A **27**, 2602 (2010).
- [69] P. Kurzynowski, W. Wozniak, M. Zdunek, M. Borwinska, *Singularities of interference of three waves with different polarization states*, Opt. Express **20**, 26755 (2012).
- [70] W. Nasalski, *Vortex and anti-vortex compositions of exact elegant Laguerre-Gaussian vector beams*, Appl. Phys. B **115**, 155 (2014).
- [71] A. M. Beckley, T. G. Brown, and M. A. Alonso, *Full Poincaré beams*, Opt. Express **18**, 10777 (2010).
- [72] F. Cardano, E. Karimi, L. Marrucci, C. de Lisio, and E. Santamato, *Generation and dynamics of optical beams with polarization singularities*, Opt. Express **21**, 8815 (2013).
- [73] E. J. Galvez, S. Khadka, W. H. Schubert, and S. Nomoto, *Poincaré-beam patterns produced by nonseparable superpositions of Laguerre-Gauss and polarization modes of light*, Appl. Opt. **51**, 2925 (2012).
- [74] G. Milione, H. I. Sztul, D. A. Nolan, R. R. Alfano, *Higher-order Poincaré sphere, Stokes parameters, and the angular momentum of light*, Phys. Rev. Lett. **107**, 053601 (2011).
- [75] V. Shvedov, P. Karpinski, Y. Sheng, X. Chen, W. Zhu, W. Krolikowski, C. Hnatovsky, *Visualizing polarization singularities in Bessel-Poincaré beams*, Opt. Express, **23**, 12444 (2015).
- [76] X. Ling, X. Yi, Z. Dai, Y. Wang, and L. Chen, *Characterization and manipulation of full Poincaré beams on the hybrid Poincaré sphere*, J. Opt. Soc. Am. B **33**, 2172 (2016).
- [77] E. J. Galvez, B. Khajavi, *Monstar disclinations in the polarization of singular optical beams*, J. Opt. Soc. Am. B **34**, 568 (2017).
- [78] M. V. Berry, and J. H. Hannay, *Umbilic points on Gaussian random surfaces*, J. Phys. A: Math. Gen. **10**, 1809 (1977).
- [79] J. F. Nye, *Natural Focusing and Fine Structure of Light*, (CRC Press, 1999).
- [80] W. Zhu, V. Shvedov, W. She, W. Krolikowski, *Transverse spin angular momentum of tightly focused full Poincaré beams*, Opt. Express **23**, 34029 (2015).